Arabian Journal of Chemistry (2011) 4, 185–193

King Saud University

Arabian Journal of Chemistry

www.ksu.edu.sa
www.sciencedirect.com

ORIGINAL ARTICLE

Employing electrochemical frequency modulation for studying corrosion and corrosion inhibition of copper in sodium chloride solutions

N.A. Al-Mobarak [a], K.F. Khaled [b,c,*], Mohamed N.H. Hamed [d], K.M. Abdel-Azim [b]

[a] Chemistry Department, Faculty of Science, Princess Nora bint Abdulrahman University, Riyadh, Saudi Arabia
[b] Electrochemistry Research Laboratory, Chemistry Department, Faculty of Education, Ain Shams University, Roxy, Cairo, Egypt
[c] Materials and Corrosion Laboratory, Chemistry Department, Faculty of Science, Taif University, Taif, Hawiya 888, Saudi Arabia
[d] Chemistry Department, Faculty of Education, Ain Shams University, Roxy, Cairo, Egypt

Received 6 May 2010; accepted 12 June 2010
Available online 25 June 2010

KEYWORDS

Copper, acid inhibition;
Pyrimidene derivative;
EFM;
EIS;
Polarization

Abstract The inhibition effect of 2-carboxymethylthio-4-(*p*-methoxyphenyl)-6-oxo-1,6-dihy-dropyrimidine-5-carbonitrile (CPD) towards the corrosion of copper was studied in aerated stagnant 3.5% NaCl at 25 °C using ac techniques include electrochemical frequency modulation and electrochemical impedance spectroscopy as well as potentiodynamic polarization measurements. Corrosion rates determined using electrochemical frequency modulation (EFM) which measures the non-linear behaviour of a corroding system are compared with corrosion rates obtained from traditional electrochemical techniques and show good agreement. Data obtained from EIS were analyzed to model the corrosion inhibition process through equivalent circuit. Polarization measurements showed that CPD acts as mixed-type inhibitor. The inhibition efficiency increases with an increase in the concentration of CPD. The adsorption of the inhibitor on the copper surface in the sodium chloride solution was found to obey Langmuir's adsorption isotherm. A mixed inhibition mechanism is proposed for the inhibitive effects of CPD as revealed by potentiodynamic polarization technique.

* Corresponding author at: Electrochemistry Research Laboratory, Chemistry Department, Faculty of Education, Ain Shams University, Roxy, Cairo, Egypt.
E-mail address: khaledrice2003@yahoo.com (K.F. Khaled).

Peer review under responsibility of King Saud University.
doi:10.1016/j.arabjc.2010.06.036

Production and hosting by Elsevier

1. Introduction

Electrochemical frequency modulation technique involves a potential perturbation composed of two sine waves when applied to a corroding surface, generates current response at more frequencies than the frequencies of applied signal. Electrochemical frequency modulation (EFM) has the capability to monitor on-line corrosion within reasonable time without prior knowledge of Tafel parameters by applying a small polarizing signal. Major benefits of EFM over harmonic

impedance spectroscopy (HIS) are validation of data quality, insensitive to harmonics in the perturbation signal and, larger current response. EFM does not require prior information of Tafel parameters rather corrosion rate, Tafel parameters and causality factors are determined in a single measurement. In theory, the magnitudes of current responses at certain intermodulation frequencies are multiples of the current responses at certain harmonic frequencies. These multiples define the causality factors of EFM (Rauf and Bogaerts, 2010).

Khaled (2008a, 2009), Amin and Khaled (2010) and Abdel-Rahim et al. (2006) have investigated that EFM is a fast and non-destructive technique to measure corrosion rate without prior knowledge of Tafel slopes. They have demonstrated the results obtained by the EFM technique in good comparison with other electrochemical techniques. Kuş and Mansfeld (2006) have evaluated the EFM technique for different systems like Cu/NaCl, Al 5083/NaCl, stainless steel/NaCl and mild steel in H_2SO_4 and NaCl. They showed that this technique can be applied successfully but only in cases of high corrosion rates. EFM technique like harmonic method determines corrosion rate (Gill et al., 1983; Rao and Mishra, 1977) with the help of non-linearity in the voltage–current response of electrochemical interface. The corrosion rate and Tafel concerning parameters could be measured accurately by the EFM technique for different metals in different environments (Devay and Meszaros, 1979). Han and Song (2008) have performed EFM measurements with 0.02 and 0.05 Hz potential perturbation frequencies to determine corrosion rates. Usually the frequencies of 0.2 and 0.5 Hz are used, based on two arguments (Yeow and Hibbert, 1983). Decreasing or increasing these frequencies to one decimal point hardly influence the results. At longer exposed times when diffusion-controlled effect became obvious, the corrosion rates determined by Han were higher, but still at the same order of magnitude as those obtained with polarization curve analysis or weight loss method.

Copper has been one of the most important metals in industry owing to its high electrical and thermal conductivities, mechanical workability and its relatively noble properties. It is widely used in many applications in electronic industries and communications as a conductor in electrical power lines, pipelines for domestic and industrial water utilities including sea water, heat conductors, heat exchangers, etc. for this reason, corrosion of copper and its inhibition in a wide variety of media, particularly when they contain chloride ions, have attracted the attention of many investigators (Khaled, 2008a).

There are two main reasons for the considerable interest in this area. Firstly, chloride ions are very aggressive ions to copper and its alloys. This is due to the tendency of the chloride ion to form an unstable film, CuCl and soluble chloride complexes, $CuCl_2^-$, $CuCl_3^{2-}$ (Yeow and Hibbert, 1983). Copper is so sensitive to chloride ions and even trace amounts of Cl^- ions can cause corrosion problem. Secondly, copper and its alloys are almost exclusively used for piping and delivery of water for domestic and industrial purposes. These pipes are frequently employed in a medium where Cl^- ions are present (Hack and Pickering, 1991).

In spite of the relatively noble potential of copper, its corrosion takes place at a significant rate in sea water and chloride environments (Sherif and Park, 2005; El-Warraky et al., 2004)

The dissolution reaction of copper in chloride solution can be given as below:

$$Cu + Cl^- \rightleftarrows CuCl_{ads} + e^- \quad (1)$$

$$CuCl_{ads} + Cl^- \rightleftarrows CuCl_2^- \quad (2)$$

$$Cu + 2Cl^- \rightleftarrows CuCl_2^- + e^- \ (\text{slow}) \quad (3)$$

Meanwhile, copper oxide and hydroxide can be formed. The cathodic reaction consists of reduction of oxygen:

$$O_2 + 2H_2O + 4e^- \rightleftarrows 4OH^- \quad (4)$$

The insoluble corrosion products forming on the surface may slow down the rate of anodic dissolution and oxygen reduction reactions. It is already known that copper corrosion could occur in chloride solutions, via degradation of corrosion products, and complex formations with chlorides. It is explained that, the rate of anodic dissolution is proportional to the rate of diffusion of $CuCl_2^-$ into the solution, that in low chloride concentration CuCl may form at the beginning and then the dissolution will proceed in the form of $CuCl_2^-$, the presence of insoluble corrosion products on the metal surface will not be able to prevent the reduction of oxygen (Kabasakaloğlu et al., 2002; Wang et al., 2004).

One of the most important methods in the protection of copper against corrosion is the use of organic inhibitors (Khaled and Hackerman, 2004).

El-Sayed M. Sherif, investigated the influence of 5-(phenyl)-4H-1,2,4-triazole-3-thiole (PTAT) Sherif and Park, 2006 in NaCl solution. It is expected that this compound shows high inhibition efficiency since they are heterocyclic compounds containing more donor atoms, besides that they are non-toxic and cheap. Substituted uracils are studied as copper corrosion inhibitors in 3% NaCl (Dafali et al., 2003). These derivatives include: uracil (Ur); 5,6-dihydrouracil (DHUr); 5-amino-uracil (AUr); 2-thiouracil (TUr); 5-methyl-thiouracil (MTUr); dithiouracil (DTUr), so the substituent influence can be estimated. Zucchi and Trabanelli (1996) studied the inhibiting action of tetrazole derivatives in 0.1 M NaCl solution. The following compounds are tested: tetrazole (T), 5-mercapto-1-methyl-tetrazole (5Mc-1Me-T), 5-mercapto(Na salt)-1-methyl-tetrazole (5NaMc-1Me-T), 5-mercapto-1-acetic acid (Na salt)-tetrazole (5Mc-1Ac-T), 5-mercapto-1-phenyl-tetrazole (5Mc-1Ph-T), 5-phenyl-tetrazole (5Ph-T) and 5-amino tetrazole ($5NH_2$-T) in the range of pH from 4 to 8 and at temperatures of 40 and 80 °C.

In continuation of our previous work on evaluation of EFM as an efficient corrosion monitoring technique as well as the development of new corrosion inhibitors for NaCl solutions (Abdel-Rahim et al., 2006; Khaled, 2003), corrosion inhibition data will be calculated using EFM technique and it will be compared with that obtained from traditional electrochemical techniques like potentiodynamic polarization and EIS measurements.

In this work, EFM measurements were used to study the corrosion and corrosion inhibition of copper in 3.5% NaCl using a new synthesized pyrimidine derivative, namely 2-carboxymethylthio-4-(*p*-methoxyphenyl)-6-oxo-1,6-dihy-dropyrimidine-5-carbonitrile (CPD), in order to evaluate the EFM as an efficient tool for online monitoring of corrosion rate in Cu/NaCl systems, which might be helpful for online application of electrochemical techniques.

2. Experimental

In this study a new pyrimidine heterocyclic derivative, namely 2-carboxymethylthio-4-(*p*-methoxyphenyl)-6-oxo-1,6-dihy- dropyrimidine-5-carbonitrile (CPD) was prepared in our laboratory where a mixture of 2-mercapto-4-(*p*-methoxyphenyl)-6-oxo-1,6-dihydropyrimidine-5-carbonitrile (0.01 mole) and chloroacetic acid (0.01 mole) in ethanolic potassium hydroxide solution (prepared by dissolving 0.56 g, 0.01 mole of KOH in 50 ml ethanol) was heated under reflux for 5 h. The solid obtained upon dilution with water was filtered off and re-crystallized from methanol to give CPD as yellow crystals with yield of 85%, m.p. 210 °C (Ram, 1984) and its chemical structure presented below:

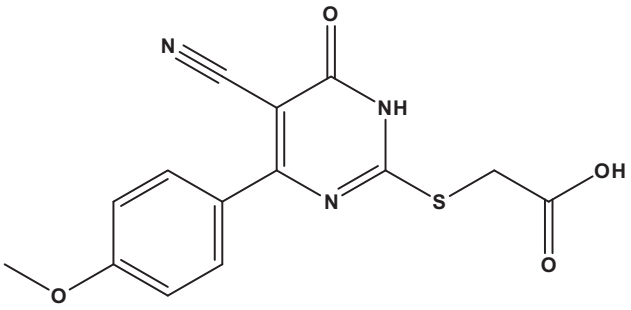

The CPD is added to the 3.5% NaCl at concentrations of 5×10^{-5}, 10^{-4}, 5×10^{-4} and 10^{-3} M.

Cylindrical rods of copper specimens obtained from Johnson Mattey (Puratronic, 99.999%) were mounted in Teflon. An epoxy resin was used to fill the space between Teflon and copper electrode. The circular cross sectional area of the copper rod exposed to the corrosive medium, used in electrochemical measurements, was (0.28 cm^2).

The electrochemical measurements were performed in a typical three-compartment glass cell consisted of the copper specimen as working electrode (WE), platinum counter electrode (CE), and a saturated calomel electrode (SCE) as the reference electrode. The counter electrode was separated from the working electrode compartment by fritted glass. The reference electrode was connected to a Luggin capillary to minimize IR drop. Solutions were prepared from double-distilled water of resistivity 13 MΩ cm, the copper electrode was abraded with different grit emery papers up to 4/0 grit size, cleaned with acetone, washed with double-distilled water and finally dried.

Tafel polarization curves were obtained by changing the electrode potential automatically from −650 to +300 mV_{SCE} at open circuit potential with scan rate of 1.0 mV s^{-1}. Impedance measurements were carried out in frequency range from 100 kHz to 40 mHz with an amplitude of 10 mV peak-to-peak using ac signals at open circuit potential. Electrochemical frequency modulation, EFM, was carried out using two frequencies 2 Hz and 5 Hz. The base frequency was 1 Hz, so the waveform repeats after 1 s. The higher frequency must be at least two times the lower one. The higher frequency must also be sufficiently slow that the charging of the double layer does not contribute to the current response. Often, 10 Hz is a reasonable limit.

The electrode potential was allowed to stabilize 60 min before starting the measurements. All experiments were conducted at 25 ± 1 °C. Measurements were performed using Gamry Instrument Potentiostat/Galvanostat/ZRA. This includes a Gamry framework system based on the ESA400, Gamry applications that include dc105 for dc corrosion measurements, EIS300 for electrochemical impedance spectroscopy and EFM 140 for electrochemical frequency modulation measurements along with a computer for collecting data. Echem Analyst 5.58 software was used for plotting, graphing and fitting data.

3. Results and discussion

3.1. Electrochemical frequency modulation, EFM

Electrochemical frequency modulation is a nondestructive corrosion measurement technique that can directly give values of the corrosion current without prior knowledge of Tafel constants. Like EIS, it is a small ac signal. Unlike EIS, however, two sine waves (at different frequencies) are applied to the cell simultaneously. Because current is a non-linear function of potential, the system responds in a non-linear way to the potential excitation. The current response contains not only the input frequencies, but also contains frequency components which are the sum, difference, and multiples of the two input frequencies. The two frequencies may not be chosen at random. They must both be small, integer multiples of a base frequency that determines the length of the experiment.

Intermodulation spectra obtained from EFM measurements are presented in Fig. 1. Each spectrum is a current response as a function of frequency. The two large peaks are the response to the 2 Hz and 5 Hz excitation frequencies. These peaks are used by the EFM140© software package to calculate the corrosion current and the Tafel constants. It is important to note that between the peaks the current response is very small. There is nearly no response (< 100 nA) at 4.5 Hz, for example, the frequencies and amplitudes of the peaks are not coincidences. They are direct consequences of the EFM theory.

Corrosion kinetic parameters are calculated from EFM techniques using the following equations (Khaled, 2008a):

$$i_{\text{corr}} = \frac{i_\omega^2}{\sqrt{482 i_\omega i_{3\omega} - i_{2\omega}}} \tag{5}$$

$$\beta_a = \frac{i_\omega U_o}{2i_{2\omega} + 2\sqrt{3}\sqrt{2i_{3\omega}i_\omega - i_{2\omega}^2}} \tag{6}$$

$$\beta_c = \frac{i_\omega U_o}{2\sqrt{3}\sqrt{2i_{3\omega}i_\omega - i_{2\omega}^2 - 2i_{2\omega}}} \tag{7}$$

$$\text{Causality factor } (2) = \frac{i_{\omega_2\pm\omega_1}}{i_{2\omega_1}} = 2.0 \tag{8}$$

$$\text{Causality factor } (3) = \frac{i_{2\omega_2\pm\omega_1}}{i_{3\omega_1}} = 3.0, \tag{9}$$

where i is the instantaneous current density at the working electrode measured at frequency ω and U_o amplitude of the sine wave distortion.

Table 1 shows the corrosion kinetic parameters such as inhibition efficiency, corrosion current density (μA/cm^2), Tafel

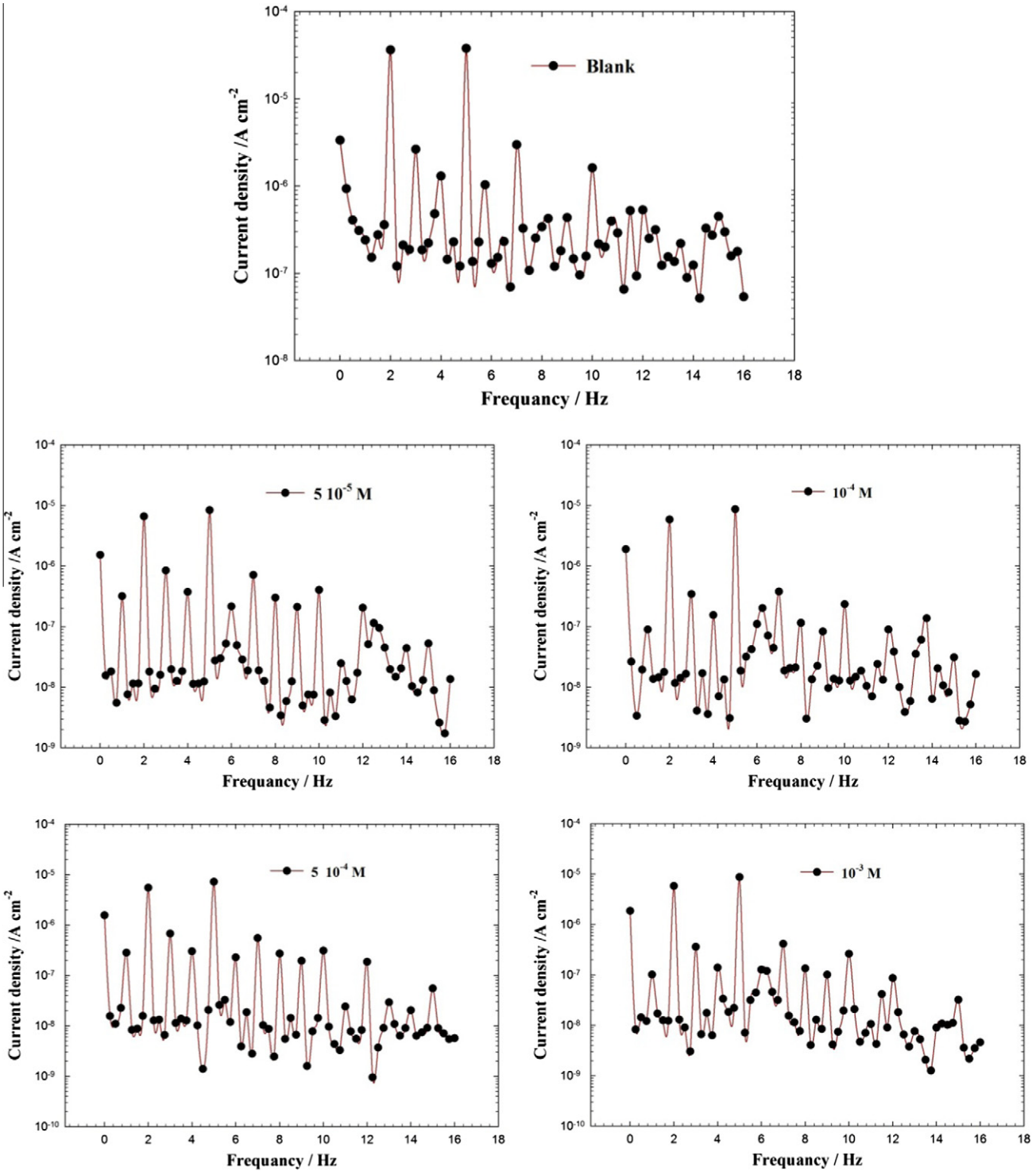

Figure 1 Intermodulation spectra recorded for copper electrode in 3.5% NaCl solutions in the absence and presence of various concentrations of CPD at 25 ± 1 °C.

constants (β_a, β_c) and causality factors (CF-2, CF-3) at different concentration of CPD derivative in 3.5% NaCl at 25 °C.

From Table 1, the corrosion current densities decrease by increasing the concentrations of CPD. The inhibition efficiencies increase by increasing CPD concentrations. The causality factors in Table 1 are very close to theoretical values which according to the EFM theory (Bosch et al., 2001) should guarantee the validity of Tafel slopes and corrosion current densities. Inhibition efficiency ($\rho_{EFM}\%$) depicted in Table 1 calculated from the following equation:

$$\rho_{EFM}\% = \left(1 - \frac{i_{corr}}{i^{o}_{corr}}\right) \times 100, \tag{10}$$

Table 1 Electrochemical kinetic parameters obtained by EFM technique for copper in 3.5% NaCl with various concentrations of CPD at 25 ± 1 °C.

	Concentration (M)	i_{corr} (μA cm^{-2})	β_a (mV$_{SCE}$ dec^{-1})	β_c (mV$_{SCE}$ dec^{-1})	C.R. (mpy)	ρ_{EFM} (%)	CF-2	CF-3
	Blank	71.7	71.7	119.1	117.1	–	1.9	1.4
CPD	5×10^{-5}	8.95	59.80	83.7	14.01	87.53	1.87	2.75
	10^{-4}	7.81	53.14	77.5	13.21	89.11	2.00	2.14
	5×10^{-4}	6.41	90.32	142.4	10.92	91.07	1.85	1.97
	10^{-3}	4.69	85.25	118.5	9.74	93.46	1.96	2.33

where i^o_{corr} and i_{corr} are corrosion current density in the absence and presence of the studied compounds, respectively.

The great strength of the EFM is the causality factors which serve as an internal check on the validity of the EFM measurement (Bosch and Bogaerts, 1996). With the causality factors the experimental EFM data can be verified. The causality factors in Table 1 indicate that the measured data are of good quality. The standard values for CF-2 and CF-3 are 2.0 and 3.0, respectively. To evaluate the EFM technique as an effective corrosion monitoring technique, several traditional corrosion techniques implied to study the corrosion inhibition of copper by CPD derivative in 3.5% NaCl solutions. EIS, Tafel extrapolation and weight loss measurements are used to calculate the inhibition efficiency as well as other corrosion kinetic parameters.

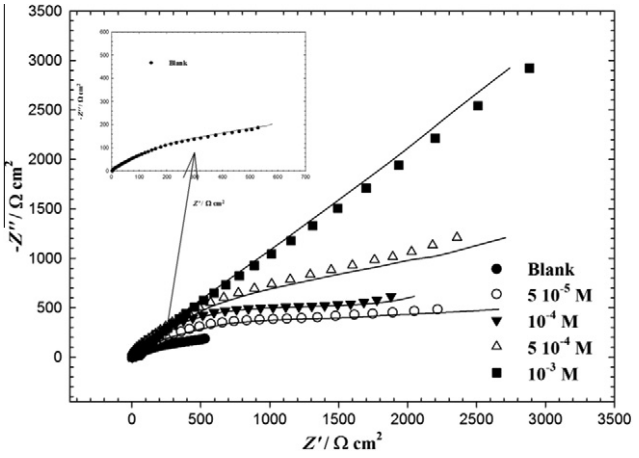

Figure 2 Nyquist plots for copper in 3.5% NaCl solutions in the absence and presence of various concentrations of CPD at 25 ± 1 °C.

3.2. Electrochemical impedance spectroscopy (EIS)

Nyquist plots recorded for copper electrode in 3.5% NaCl solutions and containing various concentrations of CPD derivative are shown in Fig. 2. As can be seen from Fig. 2, the Nyquist plots do not yield perfect semicircles as expected from the theory of EIS. The deviation from ideal semicircle was generally attributed to the frequency dispersion (El Achouri et al., 2001) as well as to the inhomogenities of the surface and mass transport resistant (Khaled and Hackerman, 2004). The shape of the impedance diagrams of copper in 3.5% NaCl is similar to those found in the literature (Khaled, 2008b). The presence of CPD increases the impedance but does not change the other aspects of corrosion mechanism occurred due to its addition. Symbols in Fig. 2 represent the measured data and solid lines represent the fitting data obtained using the equivalent circuit (Sherif and Park, 2006) presented in Fig. 3.

An equivalent circuit, such as shown in Fig. 3, was used to consider all the process involved in the electrical response of the system. R_s represents the solution resistance, R_p is the polarization resistance and can be defined also as the charge-transfer resistance, CPE_1 and CPE_2 are constant phase elements (CPEs), R'_p is another polarization resistance and W, is a Warburg impedance. The different elements were evaluated by a fitting procedure.

A constant phase element (CPE) instead of a capacitive element is used in Fig. 3 to get a more accurate fit of experimental

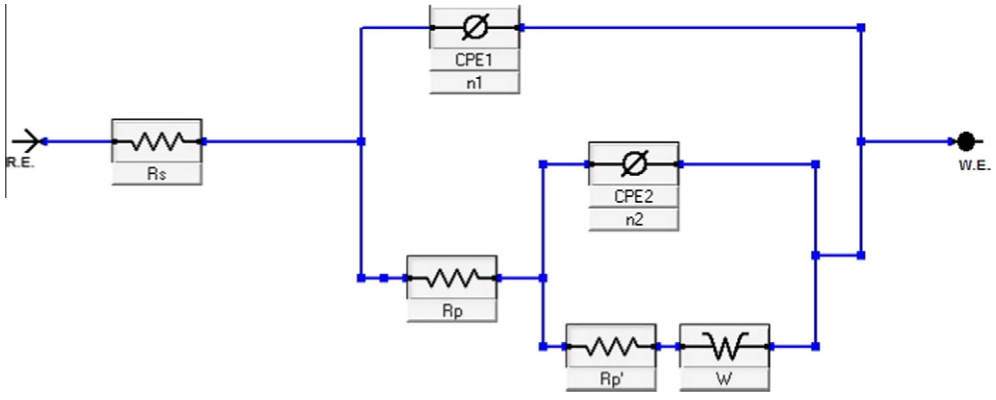

Figure 3 Equivalent circuit used to model impedance data for copper in 3.5% NaCl solutions in the absence and presence of various concentrations of CPD at 25 ± 1 °C.

Table 2 Electrochemical parameters calculated from EIS measurements on copper electrode in 3.5% NaCl solutions without and with various concentrations of CPD derivatives 25 ± 1 °C using equivalent circuit presented in Fig. 3.

Inhibitor	Concentration	M	R_s (Ω cm^2)	R_p (Ω cm^2)	CPE$_1$ (Ω^{-1} cm^{-2} s_1^n)	n_1	R'_p (Ω cm^2)	CPE$_2$ (Ω^{-1} cm$^{-2}s_2^n$	n_2	W (Ω^{-1} cm^{-2} s$^{1/2}$)	τ_{EIS} (%)
	Blank	113	733	1.3	0.89	6.1	13.5		0.52	20.3	–
CPD	5×10^{-5}	99.0	733	1.3	0.89	6.1	13.5		0.52	16.1	79.4
	10^{-4}	87.9	3434	0.88	0.85	8.2	9.8		0.55	13.4	81.3
	5×10^{-4}	90.6	3582	0.76	0.76	9.7	6.2		0.61	8.6	84.3
	10^{-3}	96.9	4339	0.54	0.73	12.3	4.2		0.56	4.5	89.9

data sets using generally more complicated equivalent circuits. The impedance, Z, of CPE has the form (Abdel-Rahim et al., 2006):

$$Z_{CPE} = [Q(j\omega)^n]^{-1}, \tag{11}$$

where Q is the CPE constant, which is a combination of properties related to the surface and electro-active species, $j^2 = -1$ the imaginary number, ω the angular frequency and n is a CPE exponent which can be used as a measure of the heterogeneity or roughness of the surface. Depending on the value of n, CPE can represent resistance ($n = 0$, $Q = 1/R$), capacitance ($n = 1$, $Q = C$), inductance ($n = -1$, $Q = 1/L$) or Warburg impedance ($n = 0.5$, $Q = W$).

The parameters obtained by fitting the experimental data using the equivalent circuit, and the calculated inhibition efficiencies are listed in Table 2. The Nyquist plots presented in Fig. 2 clearly demonstrate that the shapes of these plots for inhibited copper electrode are not substantially different from those of uninhibited electrode. Addition of CPD molecules increases the impedance but does not change other aspects of the electrode behaviour.

Parameters derived from EIS measurements and inhibition efficiency is given in Table 2. Addition of CPD increases the values of R_p and R'_p, and lowers constants of CPE$_1$ and CPE$_2$ and this effect is seen to be increased as the concentrations of CPD increase. The constant phase elements (CPEs) with their n values $1 > n > 0$ represent double layer capacitors with some pores (Sherif and Park, 2006). The CPEs decrease upon increase in CPD concentrations, which are expected to cover the charged surfaces and reducing the capacitive effects. This decrease in (CPE) results from a decrease in local dielectric constant and/or an increase in the thickness of the double layer, suggested that CPD molecules inhibit the copper corrosion by adsorption at the copper/NaCl interface The semicircles at high frequencies in Fig. 2 are generally associated with the relaxation of electrical double layer capacitors and the diameters of the high frequency semicircles can be considered as the charge-transfer resistance ($R_{ct} = R_p$) Ma et al., 2002. Therefore, the inhibition efficiency, τ_{EIS}% of CPD for the copper electrode can be calculated from the charge-transfer resistance as follows (Ma et al., 2002):

$$\tau_{EIS}\% = \left(1 - \frac{R_p^o}{R_p}\right) \times 100, \tag{12}$$

where R_p^o and R_p are the polarization resistances for uninhibited and inhibited solutions, respectively. The CPEs are almost like Warburg impedance with their n values close to 0.5 in presence of CPD (Sherif and Park, 2006), which suggests that the electron transfer reaction corresponding to the second semicircle takes place through the surface layer and limits the mass transport (Warburg). The presence of the CPE constant related to Warburg (W) impedance in the circuit confirms also that the mass transport is limited by the surface passive film. The values of copper system could be interpreted as follows: the double layer capacitance were in the range (1.3–0.54 Ω^{-1}cm^{-2}s^{n_1}), and simulated as a constant phase element (CPE$_1$) with n_1 value close to 0.8, indicating that the behaviour corresponds to a capacitor with some imperfections, such as rough and porous. The first resistance R_p corresponds to the oxidation of the metal, after this oxidation a copper oxides film is formed. This film has a higher resistance due to passive characteristics. The capacity CPE$_2$ of this film was simulated as a constant phase element too, with n_2 value close to 0.5, indicating the porous nature of the film (Vera et al., 2008). The presence of CPD on the copper surface, both resistances increase. The first resistance R_p increases as a consequence of the presence of the oxide film, which avoids the penetration of the electrolyte to the copper surface. The second resistance R'_p is the resistance of the CPD film. The capacity of the coated copper electrode is lower than the bare electrode, due to the presence of the film, which decreases the amount of the electrolyte in contact with the copper metal. From the values of R_p and R'_p it is possible to estimate the inhibition efficiency of the CPD on the copper surface as described earlier in Eq. (12).

3.3. Potentiodynamic polarization measurements

Fig. 4 shows typical polarization curves for copper in chloride media. The three distinct regions that appeared were the active dissolution region (apparent Tafel region), the active-to-

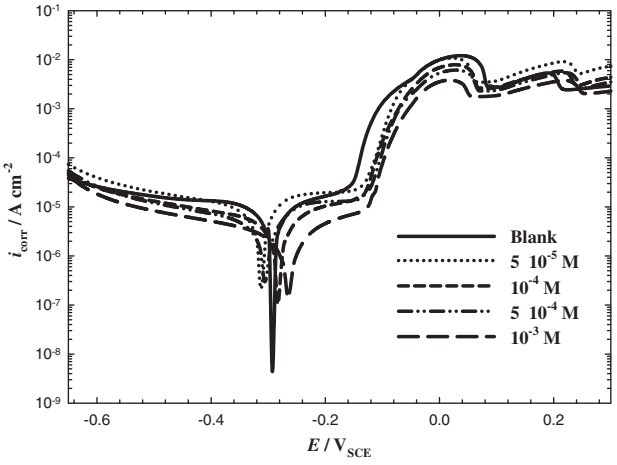

Figure 4 Anodic and cathodic polarization curves for copper in 3.5% NaCl solutions in the absence and presence of various concentrations of CPD at 25 ± 1 °C.

Table 3 Electrochemical kinetic parameters obtained by potentiodynamic technique for copper in 3.5% NaCl without and with various concentrations of CPD at 25 ± 1 °C.

	Concentration (M)	i_{corr} (μA cm^{-2})	$-E_{corr}$ (mV$_{SCE}$)	β_a (mV$_{SCE}$ dec^{-1})	δ_p (%)	θ
	Blank	11.3	293	227	–	–
CPD	5×10^{-5}	6.04	293	211.4	78.66	0.79
	10^{-4}	5.79	276	181.1	79.54	0.80
	5×10^{-4}	4.78	285	213.9	83.11	0.83
	10^{-3}	3.32	255	173.0	88.27	0.88

passive transition region, and the limiting current region. In the inhibitor-free solution, the anodic polarization curve of copper (blank-curve in Fig. 4) showed a monotonic increase of current with potential until the current reached the maximum value. After this maximum current density value, the current density declined rapidly with potential increase, forming an anodic current peak that was related to CuCl film formation.

In the presence of CPD, both the cathodic and anodic current densities were greatly decreased over a wide potential range from −650 to +300 mV$_{SCE}$. It was found from Fig. 4 that CPD had a much greater influence on the anodic current in 3.5%NaCl solution than that on the cathodic current.

It is also seen that increasing the CPD concentrations, decreases the cathodic, anodic and corrosion currents (i_{corr}) and consequently the corrosion rates.

Inspection of polarization curves in Fig. 4 shows that the anodic dissolution of copper in aerated 3.5% NaCl solutions obeys Tafel's law. The anodic curve is, therefore preferred over the cathodic one for evaluation of corrosion currents, i_{corr}, by the Tafel extrapolation method. However, the cathodic polarization curve deviate from Tafel behaviour and exhibiting a limiting diffusion current which may be due to the reduction of dissolved oxygen. This is the reason why values of the cathodic Tafel slopes, calculated from the software, are not included here.

Addition of 10^{-3} M of CPD reduces to a great extent the cathodic and anodic currents, i_{corr}. The corresponding electrochemical kinetics parameters such as corrosion potential (E_{corr}), anodic Tafel slopes (β_a) and corrosion current density (i_{corr}), obtained by extrapolation of the Tafel lines are presented in Table 3. The inhibitor efficiency was evaluated from dc measurements using Eq. (13) (Hack and Pickering, 1991):

$$\delta_p\% = \left(1 - \frac{i_{corr}}{i^{o}_{corr}}\right) \times 100, \tag{13}$$

where i^{o}_{corr} and i_{corr} correspond to uninhibited and inhibited current densities, respectively.

Inspection of Table 3 shows that the addition of different concentration of CPD decreases corrosion current densities and increases the inhibition efficiencies δ_p%.

3.4. Adsorption considerations

Important information about the interaction between the inhibitors and metal surface can be provided by adsorption isotherm. During corrosion inhibition of metals, the nature of inhibitor on the corroding surface has been deduced in terms of adsorption characteristics of inhibitor.

Organic molecules inhibit the corrosion by adsorption at the metal surface (Gil et al., 2004). Theoretically, the adsorption process has been regarded as a simple substitution process, in which an inhibitor molecule $Inh_{(aq.)}$ in the aqueous phase substitutes an "x" number of water molecules adsorbed on the metal surface vis,

$$Inh_{(aq.)} + xH_2O_{(sur)} \Longleftrightarrow Inh_{(surface)} + xH_2O \tag{14}$$

where x has been termed as the size ratio and is simply the number of water molecules replaced by one inhibitor molecule (Qiu et al., 2005). The adsorption depends on the structure of the inhibitor, the nature of the metal surface, the temperature and the electrochemical potential at the metal-solution interface.

A direct relationship between inhibition efficiency of the heterocyclic pyrimidine derivative CPD and the degree of surface coverage (θ) [Inhibition efficiency = $100\times\theta$] can be assumed for the different concentrations of the CPD. The degree of surface coverage (θ) for the different concentrations of CPD has been evaluated from the potentiodynamic polarization measurements in 3.5% NaCl at 25 ± 1 °C. The data were tested graphically by fitting to various adsorption isotherms including Freundlich, Temkin, Flory–Huggins, Bockris–Swinkles, Langmuir and Frumkin isotherms. The correlation coefficient (R^2) was used to determine the best fit isotherm which was obtained for Langmuir. According to this isotherm, θ is related to the inhibitor concentration by the following Eq. (15) (Morad and Kamal El-Dean, 2006).

$$\frac{C}{\theta} = \frac{1}{K_{ads}} + C, \tag{15}$$

where θ is the surface coverage, C is the concentration, K_{ads} is the equilibrium constant of adsorption process. K_{ads} is related

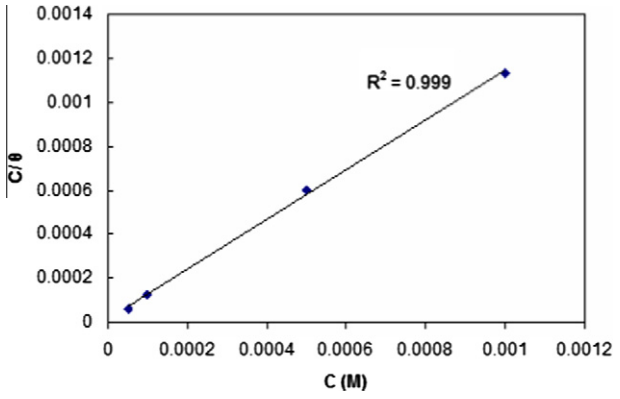

Figure 5 Langmuir adsorption isotherm of Cu in 3.5% NaCl containing CPD at 25 ± 1 °C.

to the standard Gibbs free energy of adsorption ΔG^{o}_{ads} by the Eq. (16) (Gharebaa and Omanovic, 2010).

The data was obtained from Fig. 5. The intercept of the lines in Fig. 5 yielded K_{ads} in ($dm^3\ mol^{-1}$), and the corresponding standard Gibbs free energy of adsorption in (kJ mol^{-1}) was then calculated from Eq. (16) (Sethi et al., 2007):

$$K_{asd} = \frac{1}{C_{sovent}} \exp\left(\frac{-\Delta G^{o}_{ads}}{RT}\right), \quad (16)$$

where R in (J $mol^{-1}\ K^{-1}$) is the gas constant, T (K) is the temperature, and C_{sovent} is the molar concentration of the solvent, which in this case, is water ($C_{H_2O} = 55.5$ mol dm^{-3}). Using this equation, the various adsorption parameters are obtained from the studied isotherm including the standard Gibbs free energy of adsorption of CPD on copper surface. Fig. 5 shows the plot of C/θ vs. C and linear plot was obtained for CPD derivative indicating that the adsorption of CPD molecules followed Langmuir isotherm. The various adsorption parameters obtained from this isotherm are listed in Table 4. It is seen from Table 4 that the correlation coefficients are very good and K_{ads} values increases with increasing inhibitor concentration showing that the molecules of the inhibitors were adsorbed on the copper surface. Although the plots are linear as depicted by R^2 values (0.99) however, the slopes deviates from the value of unity as expected from the ideal Langmuir adsorption equation. This deviation may be explained on the basis of the interaction among adsorbed CPD molecules on the copper surface. It has been postulated in the derivation of Langmuir isotherm equation that adsorbed molecules do not interact with one another, but this is not true in the case of large organic molecules having polar atoms or groups which can adsorbed on the cathodic and anodic sites of the metal surface. Such adsorbed species interact by mutual repulsion or attraction. It is also possible that the inhibitor studied can be adsorbed on the anodic and cathodic sites resulting in deviation from unit gradient. Similar observation has been reported in the literature (Sethi et al., 2007; Migahed et al., 2003).

Results presented in Table 4, indicate that the values of ΔG^{o}_{ads} are negative and equals -26 kJ mol^{-1}.The negative values signify adsorption of the CPD molecules via mixed adsorption mechanism. It is also seen that the values of ΔG^{o}_{ads} increased with an increase in inhibitor concentrations, a phenomenon which indicates that the adsorption of the inhibitor onto copper surface was favorable with increasing CPD concentrations.

Literature demonstrates that values of standard Gibbs free energy of adsorption in aqueous solution around -20 kJ mol^{-1} or lower (more positive) indicate adsorption with electrostatic interaction between the adsorbent and adsorbate (physisorption), while those around or higher (more negative) than -40 kJ mol^{-1} involve charge sharing between the molecules and the metal (chemisorption) Bilgic and Sahin, 2001. However, this should be taken with caution since the enthalpy of adsorption is the parameter that actually reflects the adsorption bond strength, rather than the standard Gibbs free energy of adsorption (Gharebaa and Omanovic, 2010).

Table 4 Inhibitor binding constant (K_{ads}), free energy of adsorption (ΔG^{0}_{ads} kJ/mol) CPD in 3.5% NaCl at 25 ± 1 °C, using potentiodynamic polarization measurements.

Inhibitor	Langmuir	
	ΔG^{0}_{ads} (kJ/mol)	K_{ads} ($dm^3\ mol^{-1}$)
CPD	−26.76	50,000

3.5. Inhibition mechanism

Adsorption of CPD molecules can be described by two main types of interactions: physical adsorption and chemisorption. In general, physical adsorption requires the presence of both the electrically charged surface of the metal and charged species in solution.

A chemisorptions process, on the other hand, involves charge sharing or charge-transfer from the inhibitor molecules to the metal surface to form a coordinate type of a bond. This is possible in case of a positive as well as a negative charge of the surface. The presence of a transition metal, having vacant, low-energy electron orbitals (Cu^{+} and Cu^{2+}) and of an inhibitor with molecules having relatively loosely bound electrons or hetero-atoms with a lone pair of electrons is necessary (Thomas, 1980).

In neutral NaCl solutions, pyrimidine heterocyclic derivative, CPD may be adsorbed on the copper surface in the form of neutral molecules involving the displacement of water molecules from the metal surface and sharing of electrons between the nitrogen atoms and the metal surface (chemical adsorption).

Also, the presence of pyrimidine heterocyclic derivative, CPD molecules may induce the formation of semi conductive copper oxides as in case of benzotriazoles (Baba and Kodama, 1999). This was possibly responsible for the improvement of corrosion resistance.

The type of intermediates that formed on Cu surface in 3.5% NaCl can be explained according to the potential-pH diagram. The presence of Cu_2O may facilitate adsorption via H-bond formation. Another possible mechanism, therefore may be adsorption assisted by hydrogen bond formation between unprotonated N, O and S atoms in pyrimidine heterocyclic derivatives molecule and the oxidized surface (Cu_2O) species. Unprotonated N, O and S atoms may adsorb by direct chemical adsorption or by hydrogen bonding to a surface oxidized species. The extent of adsorption by the respective modes depends on the nature of the metal surface. The adsorption layer acts as an additional barrier to the corrosive attack and enhances the performance of the passive layer as a result.

The criteria for inhibitor selection can also be inferred from above considerations. A good inhibitor must have strong affinity for the bare metal atoms. The requirement is different in the presence of the oxide species, a passive oxide film is formed on the electrode surface, where hydrogen bond formation accounts for most of the inhibition action. An effective inhibitor is one that forms hydrogen bonds easily with the oxidized surface. These findings could be further explained on the basis that in presence of dissolved oxygen (Amin and Khaled, 2010), where the metal surface is oxidized, the ability of a pyrimidine heterocyclic derivative, CPD to provide corrosion inhibition is related to its tendency to form hydrogen bonds with the oxide species on the metal surface. It is quite evident from the chemical structure of pyrimidine heterocyclic derivative molecule, CPD that it has NH bonds. These results confirmed the importance of hydrogen bonding in effective corrosion inhibition in presence of oxide species.

4. Conclusions

Electrochemical frequency modulation EFM can be used as a rapid and non-destructive technique for corrosion rate measurements without prior knowledge of Tafel slopes. Experimental investigations showed that CPD reduces markedly the copper corrosion in 3.5% NaCl solutions, and this reduction in corrosion rates enhances with concentration of this compound. Polarization studies show that CPD acts as mixed-type inhibitors. The results of EIS indicate that the value of CPEs tends to decrease and both charge-transfer resistance and inhibition efficiency tend to increase by increasing the inhibitor concentration. This result can be attributed to increase of the thickness of the electrical double layer. The adsorption of CPD molecules on the copper surface in the sodium chloride solution was found to obey Langmuir's adsorption isotherm. A mixed inhibition mechanism is proposed for the inhibitive effects of CPD as revealed by potentiodynamic polarization technique.

References

Abdel-Rahim, S.S., Khaled, K.F., Abd-Elshafi, N.S., 2006. Electrochim. Acta 51, 3269.

Amin, M.A., Khaled, K.F., 2010. Corros. Sci. 52, 1762.

Amin, M.A., Khaled, K.F., 2010. Corros. Sci. 52, 1194.

Baba, H., Kodama, T., 1999. Corros. Sci. 41, 1987.

Bilgic, S., Sahin, M., 2001. Mater. Chem. Phys. 70, 290–295.

Bosch, R.W., Bogaerts, W.F., 1996. Corrosion 52, 204.

Bosch, R.W., Hubrecht, J., Bogaerts, W.F., Syrett, B.C., 2001. Corrosion 57, 60.

Dafali, A., Hammouti, B., Mokhlisse, R., Kertit, S., 2003. Corros. Sci. 45, 1619.

Devay, J., Meszaros, L., 1979. Acta Chim. Acad. Sci. Hung. 100, 183.

El Achouri, M., Kertit, S., Gouttaya, H.M., Nciri, B., Bensouda, Y., Perez, L., Infante, M.R., Elkacemi, K., 2001. Prog. Org. Coat. 43, 267.

El-Warraky, A., El-Shayeb, H.A., Sherif, E.M., 2004. Anti-corros. Methods Mater. 51, 52.

Gharebaa, S., Omanovic, S., 2010. Corros. Sci. 52, 2104.

Gil, P.M., Silva, G.N., Romo, M.R., Chavez, C.A., Pardave, M.P., 2004. Electrochim. Acta 49, 4733.

Gill, J.S., Callow, M., Scantlebury, J.D., 1983. Corrosion 39, 61.

Hack, H.P., Pickering, H.W., 1991. J. Electrochem. Soc. 138, 690.

Han, L., Song, S., 2008. Corros. Sci. 50, 1551.

Kabasakaloğlu, M., Kıyak, T., Şendil, O., Asan, A., 2002. Appl. Surf. Sci. 193, 167.

Khaled, K.F., 2003. Electrochim. Acta 48, 2493.

Khaled, K.F., 2008a. Mater. Chem. Phys. 112, 290.

Khaled, K.F., 2008b. Mater. Chem. Phys. 112, 104.

Khaled, K.F., 2009. J. Appl. Electrochem. 39, 429.

Khaled, K.F., Hackerman, N., 2004. Electrochem. Acta 49, 485.

Kuş, E., Mansfeld, F., 2006. Corros. Sci. 48, 965.

Ma, H., Chen, S., Niu, L., Zhao, S., Li, S., Li, D., 2002. J. Appl. Electrochem. 32, 65.

Migahed, A., Mohammed, H.M., Al-Sabagh, A.M., 2003. Mater. Chem. Phys. 80, 169–175.

Morad, M.S., Kamal El-Dean, A.M., 2006. Corros. Sci. 48, 3398.

Qiu, L.G., Xie, A.J., Shen, Y.H., 2005. Corros. Sci. 47, 273.

Ram, V.J., Berche, D.A.V., Vlietinck, A.J., 1984. J. Heterocycl. Chem. 21, 1307.

Rao, G.P., Mishra, A.K., 1977. J. Electroanal. Chem. 77, 121.

Rauf, A., Bogaerts, W.F., 2010. Corros. Sci. doi:10.1016/j.corsci.2010.04.016.

Sethi, T., Chaturvedi, A., Updhyay, R.K., Mathur, S.P., 2007. J. Chil. Chem. Soc. 52, 1206–1213.

Sherif, E.M., Park, S.-M., 2005. J. Electrochem. Soc. B 152, 428.

Sherif, E.M., Park, S.M., 2006. Corros. Sci. 48, 4065.

Thomas, J.G.N., 1980. In: Proceedings of 5th European Symposium on Corrosion Inhibitors, 1980, 1981. Ann. Univ. Ferrara, Italy, p. 453.

Vera, R., Bastidas, F., Villarroel, M., Oliva, A., Molinari, A., Ramirez, D., Rio, R., 2008. Corros. Sci. 50, 729.

Wang, C., Chen, S., Zhao, S., 2004. J. Electrochem. Soc. 151, B11.

Yeow, C.W., Hibbert, D.B., 1983. J. Electrochem. Soc. 130, 786.

Zucchi, F., Trabanelli, G., Fonsati, M., 1996. Corros. Sci. 38, 2019.